Journal of Molecular Graphics and Modelling 28 (2010) 707–713

Contents lists available at ScienceDirect

Journal of Molecular Graphics and Modelling

journal homepage: www.elsevier.com/locate/JMGM

Molecular modeling studies of L-arabinitol 4-dehydrogenase of *Hypocrea jecorina*: Its binding interactions with substrate and cofactor

Manish Tiwari [a], Jung-Kul Lee [a,b,*]

[a] Department of Chemical Engineering, Konkuk University, Seoul 143-701, Republic of Korea
[b] Institute of Biomedical Science and Technology, Konkuk University, Seoul 143-701, Republic of Korea

ARTICLE INFO

Article history:
Received 28 September 2009
Accepted 9 January 2010
Available online 18 January 2010

Keywords:
L-Arabinitol 4-dehydrogenase
Catalytic Zn^{2+}
Cofactor binding domain
Hypocrea jecorina
Molecular modeling

ABSTRACT

L-Arabinitol 4-dehydrogenase (LAD1; EC 1.1.1.12) is an enzyme in the L-arabinose catabolic pathway of fungi that catalyzes the conversion of L-arabinitol into L-xylulose. The primary objective of this work is to identify the catalytic and coenzyme binding domains of LAD1 from *Hypocrea jecorina* in order to provide better insight into the possible catalytic events in these domains. The 3D structure of NAD^+-dependent LAD1 was developed based on the crystal structure of human sorbitol dehydrogenase as a template. A series of molecular mechanics and dynamics operations were performed to find the most stable binding interaction for the enzyme and its ligands. Using the verified model, a docking study was performed with the substrate L-arabinitol, Zn^{2+} and NAD^+. This study found a catalytic Zn^{2+} binding domain (Cys66, His91, Glu92 and Glu176) and a cofactor NAD^+ binding domain (Gly202, ILeu204, Gly205, Cys273, Arg229 and Val298) with strong hydrogen bonding contacts with the substrate and cofactor. The binding pockets of the enzyme for L-arabinitol, NAD^+, and Zn^{2+} have been explicitly defined. The results from this study should guide future mutagenesis studies and provide useful clues for engineering enzymes to improve the utilization of polyols for rare sugar production.

© 2010 Elsevier Inc. All rights reserved.

1. Introduction

L-Arabinitol 4-dehydrogenase (LAD1) is the second enzyme in the L-arabinose catabolic pathway of fungi that catalyzes the reaction from L-arabinitol to L-xylulose. Previous reports suggest that Lad1 is indeed essential for catabolism of L-arabinose and is part of an essential step in the catabolism of several hexoses [1]. LAD1 catalyzed the oxidation of pentitols (L-arabinitol) and hexitols (D-allitol, D-sorbitol, L-iditol, L-mannitol) into the corresponding ketose as mammalian SDH, albeit with different catalytic efficacies with the highest k_{cat}/k_m for L-arabinitol [1]. LAD1 from *Hypocrea jecorina* consists of 377 amino acids and has a calculated molecular mass of 39,822 Da. It belongs to the family of zinc-binding dehydrogenase and has a significant amino acid sequence similarity to human sorbitol dehydrogenase (hSDH). A previous study reported that LAD1 required NAD as a cofactor when no activity was observed with NADP [2]. Another LAD from *Neurospora crassa* was characterized and found to be highly active and stable. The enzyme was a homotetramer containing two Zn^{2+} ions per subunit and displaying similar characteristics to medium-chain sorbitol dehydrogenase (SDH) [3].

In this current investigation, an NAD^+ dependent LAD1 (EC 1.1.1.12, AAL08944) from *H. jecorina* [2] was selected as a model LAD for in silico studies. Until now, the atomic level structural details of all LADs have remained unexplored. Hence, homology modeling studies were initiated with the aim of revealing the molecular architecture of the active site in the structural framework for catalysis. The three dimensional (3D) features of the LAD1 model were obtained by homology modeling based on the crystal structure of hSDH (PDB id:1PL8A) [4]. In order to understand the interactions of LAD1 with its ligands at the molecular level, a molecular simulation of the LAD1-substrate, LAD1-Zn^{2+} and LAD1-NAD^+ complex was performed using CDOCKER in Discovery Studio 2.5 (DS2.5). The information on the catalytic and binding domains of LAD1 is important to understand the action mode of the ligands and the catalytic mechanism. The molecular modeling and docking studies indicated extensive structural details. The active site, a zinc metal binding domain and cofactor NAD^+ binding domain were identified. The key residues involved in the ligand binding were also determined. Finally, the role of the individual amino acids and the catalytic mechanism for LAD1 were proposed in detail.

* Corresponding author at: Department of Chemical Engineering, Konkuk University, 1 Hwayang-Dong, Seoul 143-701, Republic of Korea.
Tel.: +82 2 450 3505; fax: +82 2 458 3504.
E-mail address: jkrhee@konkuk.ac.kr (J.-K. Lee).

1093-3263/$ – see front matter © 2010 Elsevier Inc. All rights reserved.
doi:10.1016/j.jmgm.2010.01.004

2. Materials and methods

2.1. Multiple sequence alignment

The multiple sequence alignment of fungal LAD1 and its mammalian orthologue SDH [1] sequence was performed using the Align Multiple Sequences module of DS2.5. The following included sequence for this alignment was retrieved from the National Center for Biotechnology Information (NCBI) database. Human_Sdh (46015229), Sdh_*H. sapiens* (NP_003095.2), Sdh_*M. musculus* (NP_666238.1), Sdh_*P. stipitis* (XP_001387001.1), Lad1_*A. fumigatus* (EDP56335.1), Lad1_*A. oryzae* (BAC81768.1), Lad1_*N. crassa* (28927596), Lad1_*H. jecorina* (AAL08944) (http://www.ncbi.nlm.nih.gov) (Supplementary Fig. S1). The alignment was checked for deletions and insertions into the structurally conserved regions. Also, secondary structure cartoon prediction was carried out based on Kabsch [5] secondary structure definition using the sequence analysis module. The template (1PL8A) sequence and target LAD1 sequence were aligned

2.2. Homology modeling

The 3D structure of LAD1 was generated using the MODELER [6] in DS2.5 (Accelrys Software Inc., San Diego, CA). A BLAST search of PDB indicated the significant sequence identity (43%) between LAD1 and hSDH (PDB accession code 1PL8A) possessing the highest bit score of 254.2 among all of the search results, including the protein sequence of mammalian SDH [1]. Unanimously, the crystal structure of hSDH (resolution 1.9 Å) [4] was selected as the template. The output file for the multiple sequence alignment of the target (LAD1) and template (1PL8A) was generated using the sequence analysis module of DS2.5. Before this output file served as an input for the design of the homology model, the health of this template structure was checked using the protein health module. The final model was validated using PROCHECK. The active site/binding site of *H. jecorina* LAD1 was identified using the binding site analysis tool of DS2.5, which identified several binding sites. Then these binding sites were compared with the template 1PL8A.

2.3. Molecular dynamic simulation and docking

CDOCKER was used for the docking study [7]. The CHARMm [8] force field was used for the molecular dynamics simulation and the energy minimizations in the docking process. The solvation protocol was used to create an explicitly solvated system using CHARMm with a 15 Å cap from the center of the mass of LAD1. Starting from the new ligand configuration, a set of 10 different orientations were randomly generated and placed into the receptor, meaning moved into the center of the grid. Once the randomized ligand has been docked into the active protein site, an MD simulation was performed with a gradual heating phase of 2000 1-fs steps from 300 to 700 K, followed by a cooling phase of 5000 1-fs steps back to 300 K [9]. The resulting structure was refined with a short energy minimization containing 100 steps of a smart minimizer followed by 50 steps of a conjugate gradient. Catalytic Zn^{2+} and NAD^+ were docked into the Zn^{2+} binding domain and coenzyme binding domain, respectively. The binding patterns of Zn^{2+} and NAD^+ were compared with the SDH + NAD^+ complex crystal structure (1PL8A). An energy minimized structure containing Zn^{2+} and NAD^+ was used as the receptor for substrate docking. Random substrate conformations were generated using high-temperature MD. Candidate poses were then created using random rigid-body rotations followed by simulated annealing. The structure of the protein, substrate, and their complexes were subjected to energy minimization using the CHARMm force field implemented in DS2.5. The substrate poses were then refined with a full-potential final minimization. The energy docked conformation of the substrate was retrieved for post-docking analysis based on C-DOCKER. As a result, the substrate orientation with the lowest interaction energy was chosen for another round of docking. The automated preparation of schematic diagrams was included for the protein–ligand complexes in which the ligand was displayed in the conventional 2D form, and the interactions between the residues in its vicinity were summarized in a concise manner

3. Results and discussion

3.1. Secondary structure of H. jecorina LAD1

The activity of LAD1 (1.1.1.12) from *H. jecorina* has been previously characterized [2]. The LAD1 sequence (AAL08944, GI: 15811375) was retrieved from the NCBI database. The enzyme contains 377 amino acids. The sequence alignment between the target enzyme (LAD1) for modeling and the template (1PL8A) was performed using the Align Multiple Sequences module of DS2.5. The structurally conserved regions of the model and template were determined by superimposition and pair wise alignment. The conserved characteristics of the dinucleotide-binding proteins have been described in several studies [10,11]. The common sequence feature was a glycine-rich phosphate binding loop containing three conserved glycine residues arranged in a pattern such as GXGXXG. This motif was also present within the sequence of LAD1 and was comprised of the following amino acids GAGPIG. The secondary structure cartoon of LAD1 was color coded, with helices in red, strands in blue, and coils in beige (Fig. 1).

3.2. Homology modeling of H. jecorina LAD1

Since the accuracy of the homology model is related to the degree of the sequence identity between template and target, the template search and sequence alignment are crucial steps in any homology modeling [12]. For this reason extreme caution was taken when searching for the template and aligning the sequences. Then comparative modeling was performed to generate the most probable structure of the query protein through the alignment with template sequences and simultaneously satisfying the spatial restraints and local molecular geometry. The 3D homology model of LAD1 was generated using the MODELER in DS2.5. The generated structure was improved through the subsequent refinement of the loop conformations by assessing the compatibility of an amino acid sequence to the known PDB structures using the Protein Health module in DS2.5. In this model, the structure of LAD1 subunit (Supplementary Fig. S2) closely resembled the structure of the template. The 3D structure of LAD1 was comprised of 14α helices and 18β sheets. The overall fold of the modeled LAD1 was similar to that of one hSDH subunit. The subunit of LAD1 was organized into two domains separated by a deep cleft. The catalytic domain housed the catalytic Zn^{2+} atom that was required for activity. The organization of the polypeptides chain was similar in nature to the NAD-binding domain for the other enzyme structure. The coenzyme binding domain was a classical Rossmann fold [10] binding the required NAD(H).

3.3. Model validation

For the docking study, the model was validated using PROCHECK [13] in order to confirm the consistency of the model. The Ramachandran's plot was calculated with the PROCHECK program. The calculated Ramachandran's plot suggested that 90.2%, 8.2%, 0.7%, and 1.0% of the residues in derived model were in the most favored, additional allowed, generously allowed and disallowed regions, respectively. Altogether 99.0% of the residues

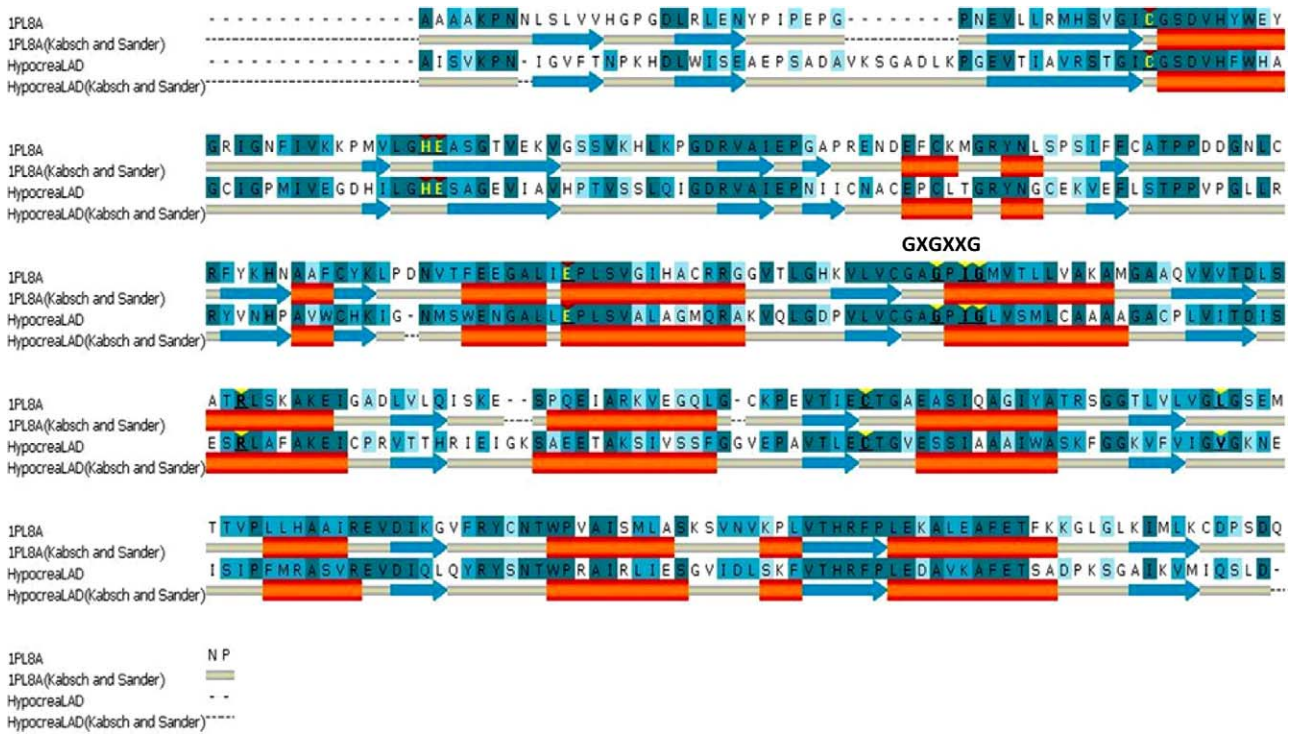

Fig. 1. The sequence alignment between *Hypocrea jecorina* LAD1 (AAL08944) and its template structure Human sorbitol dehydrogenase (1PL8A) using DS2.5. The sequence identity is 43% and the sequence similarity is 59%. The secondary structure cartoon shown is based on the Kabsch and Sander method. The secondary structure elements of LAD1 are color coded, with helices in red, strands in blue, and coils in beige.

were placed into the combined favored and allowed categories. Thus PROCHECK validated the folding integrity of the model and indicated that the model structure derived from the 1PL8A template was of higher quality in terms of protein folding. Supplementary Fig. S3 show the distribution of ϕ and φ for the Ramachandran's plot of the non-glycine, non-proline residues. The profile-3D score was also computed using the verify protein module in DS2.5 and was 147.54 on a scale with a maximum expected score of 164.97. This profile-3D score compared well to the score of 156.74 for the coordinates of 1PL8A. The build model was also evaluated by superimposing it onto the template crystal structure, and RMSD was 1.01 based on the C-alpha atoms. The generated structure improved after subsequent refinement of the loop conformations by assessing the compatibility of an amino acid sequence to the known PDB structures using the Protein Health module in DS2.5. Supporting this point, line plot graphs were plotted between verify score vs. amino acid index (Supplementary Fig. S4) and average hydrophobicity vs. residues index (Supplementary Fig. S5) for LAD1 model and template 1PL8A. And two fairly consistence profiles were observed indicating that the LAD1 model was reasonable and could be employed for further docking study.

3.4. Active site modeling

The binding site was predicted with a defined receptor molecule using the binding site tool in DS2.5. Since both the LAD1 model and template 1PL8A shared a reasonable identical sequence and structural traits, their biological functions were assumed to be similar. The catalytic residues were compared and superimposed onto the template structure. The residues in the zinc binding domain (Cys66, His91, Glu92 and Glu176) and the coenzyme binding domain (Gly202, ILeu204, Gly205, Cys273, Arg229 and Val298) of LAD1 had similar orientations and positions to the residues in the template 1PL8A (Fig. 2). As a result, the predicted site was chosen as the most favorable binding site for docking the substrate and cofactor. Thus, we suggest that the substrate and cofactor bind to LAD1 in a manner similar to hSDH, and it should facilitate the coordination of catalytic Zn^{2+} into the active site as well as facilitate the coenzyme binding.

3.5. Molecular dynamic (MD) simulation and docking

The refined and validated LAD1 model was used for the further study of docking. Hydrogen atoms were added to mimic the

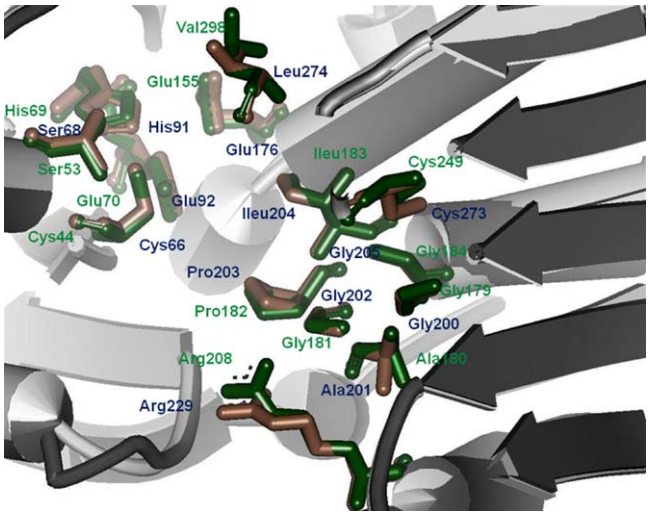

Fig. 2. Putative catalytic and coenzyme binding domain of LAD1 (orange color) superimposed on human sorbitol dehydrogenase (hSDH; 1PL8A) (green color). The LAD1 residues (Cys66, His91, Glu92 and Glu176) corresponding to the hSDH catalytic site residues and the coenzyme binding domain (Gly202, ILeu204, Gly205, Cys273, Arg229 and Val298) have similar orientations. The residues of LAD1 and hSDH are labeled with blue and green color, respectively.

proteins corresponding to the experimental pH condition. The added hydrogen atoms were energy minimized to relax the close contact conformation. The centered enzyme-substrate complex was solvated in a sphere of water molecules with a radius of 15 Å to account for the salvation effect. The structures of the protein, ligands (Zn^{2+} and coenzyme NAD^+) and their complexes were subjected to energy minimization using the CHARMm force field implemented in DS2.5. Catalytic Zn^{2+} and NAD^+ were docked to their respective binding domains one by one. Then the energy minimized complex of the enzyme, Zn^{2+} and NAD^+ was used as the receptor molecule for docking with its natural substrate L-arabinitol. The protein structure was kept rigid, and the ligand structure was flexible in the protein-substrate complex. For each ligand, 100 replicas were generated and randomly distributed around the center of the active site during every single docking run. Starting from a reasonable structure with random initial velocities for each ligand atom, a random configuration was generated for the ligand by running 1000 2-fs steps of MD at a constant temperature of 1000 K for each docking run. In the end, the final docking poses were ranked based on the total docking (CDOCKER) energy including the intra-molecular energy for the ligands and the ligand–protein interactions, and the lowest energy structure was used for post-docking analysis (Fig. 3).

3.6. Location and binding of Zn^{2+} ion

Numerous examples of homology modeling techniques have been reported that support the protein-substrate/ligand interaction, especially with respect to substrate specificity and substrate recognition [14–16]. The binding pocket of the receptor was defined within a distance of 5 Å from a heavy atom of the ligand [17]. Alcohol dehydrogenases (ADHs) are zinc metalloenzymes [18] containing two tetrahedrally coordinated zinc ions per subunit, one catalytic at the active site, and one structural site. Although the catalytic zinc binding sites were generally composed of three amino acid ligands (one His and two Cys) and a water molecule, it showed some variation for the entire ADH family. The greatest variation comes from third ligand. In the polyol dehydrogenase family, the third ligand is Glu and it can either be the residue that is adjacent to the His ligand or another Glu that is 85 residues away [19]. In the current investigation, LAD1 showed a similar residual positioning to Glu92, which was adjacent to the principle ligand His91, while another Glu176 was exactly 85 residues away. The Cys66, His91, Glu92 and Glu176 residues were involved in coordination of catalytic Zn^{2+} with liganding distances of 4, 1.8, 2, and 2 Å, respectively, along with a distance of 2.2 Å for a water molecule HOH14 (Fig. 3A). These residues formed a Zn^{2+} binding domain similar to that of hSDH (Cys44, His69, Glu70 and Glu155). The structure of whitefly NADP(H) ketose reductase had a very similar coordination of catalytic zinc with Cys41, His66, Glu67 and a water molecule linked through Glu152 [20]. Glu176 could transiently coordinate directly to the zinc atom to permit the release of the product during catalysis like Glu68 in ADH, as proposed from a computational analysis [21].

3.7. Coenzyme binding domain

In the current investigation, nucleotide-binding fold was observed, and the mode of cofactor binding appeared to be structurally conserved. Structure based studies on the sequence patterns found in the fingerprint region of the nucleotide-binding domain for a number of NAD(P)-binding proteins have identified the different requirements for nucleotide specificity. NAD^+ requires a glycine rich highly conserved GXGXXG sequence motif. This motif was also present within the sequence of LAD1 and was comprised of the following amino acids GAGPIG (Fig. 1). NAD^+

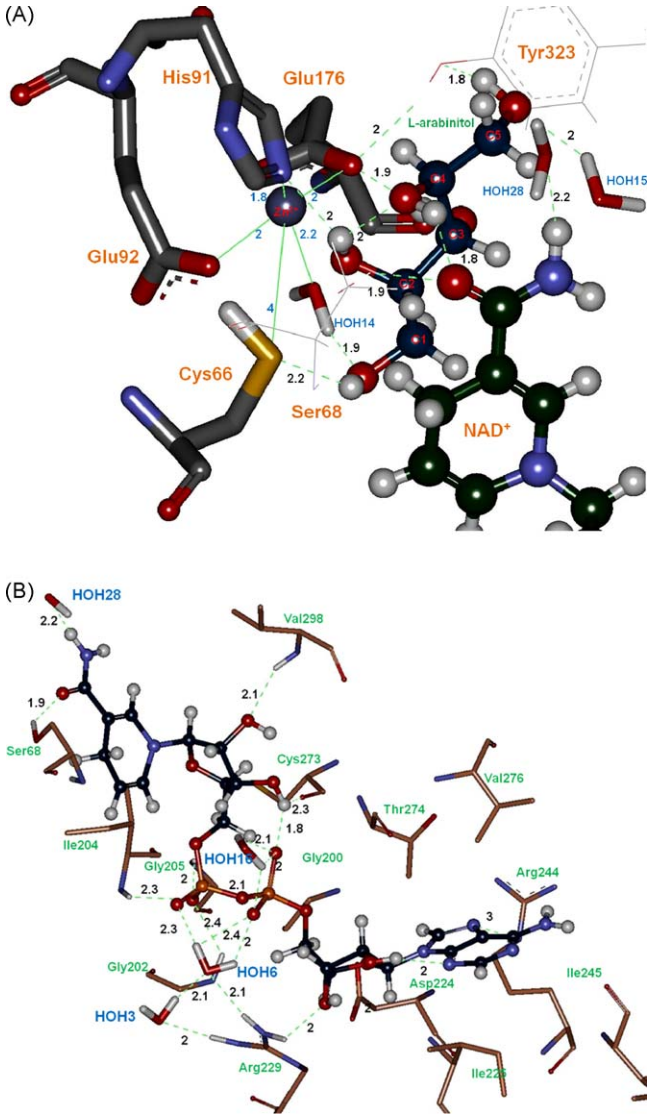

Fig. 3. (A) The binding mode of Zn^{2+} and the substrate in the putative catalytic site of LAD1. The labels indicate the residue position in LAD1. Metal ion is shown in the ball mode and the residues involved in interaction with the enzyme are represented in stick form. The L-arabinitol bound to LAD1 is shown in the ball and stick model labeled with carbon. (B) The most favorable interactions obtained for LAD1 with NAD^+ in the coenzyme binding domain from the molecular docking and MD simulations. NAD^+ is shown in the ball stick model, NAD^+ Carbon is colored dark blue. The residues involved in the interactions with NAD^+ are shown in the stick model. Hydrogen bonds are the green dashed line and the distances shown are in Å.

bound to the coenzyme binding domain with full occupancy of the available binding sites in an extended conformation across the C-terminal edge of the parallel β-sheet of the domain so that each half of the nucleotide was positioned on separate sides of the sheet. The adenosine half was in a cleft at the surface of the domain, and the nicotinamide half deep in the protein was at the active site cleft. The coenzyme binding domain residues (Gly202, ILeu204, Gly205, Cys273, Arg229 and Val298) of *H. jecorina* LAD1 are the classical rossmann fold form that reversibly binds the required NAD^+(H) [4]. The MD calculations revealed the interaction of NAD^+ with the residues involved in the coenzyme binding. Val298 (2.2 Å) and Cys273 (2.3 Å) formed hydrogen bonds with the C2′ and C3′ hydroxyl groups of ribose. Similar hydrogen bonds were observed between Gly205 (2 Å), Gly202 (2.4 Å), Ileu204 (2.3 Å) and oxygen of pyrophosphate. The C3′ hydroxyl group of the other ribose, which was associated with the adenine moiety, was hydrogen

bonded (2 Å) to the guanidinium group of Arg229 and it was also hydrogen bonded to Arg244 (3 Å) (Fig. 3B). The sequence and structural basis for the selection of NAD^+ over $NADP^+$ in dehydrogenases has been described in a previous report [22], and LAD1 fits the known pattern. The presence of an aspartic acid (in LAD1, Asp224) was the primary determinant of the NAD^+ dependency. The aspartic acid was involved in a polar interaction with hydroxyl of NAD^+ ribose (Fig. 4B) and occupied the space that would have been occupied by the phosphate attached to the 2C′ hydroxyl in $NADP^+$. Several water molecules (HOH3, HOH6, HOH16, and HOH28) were found in the interface between the dinucleotide and the protein. Water molecules formed hydrogen bonds with the dinucleotide pyrophosphate. The presence of numerous water mediating the hydrogen bonds between the protein and nucleotide implicated that water was a significant component in dinucleotides recognition [23].

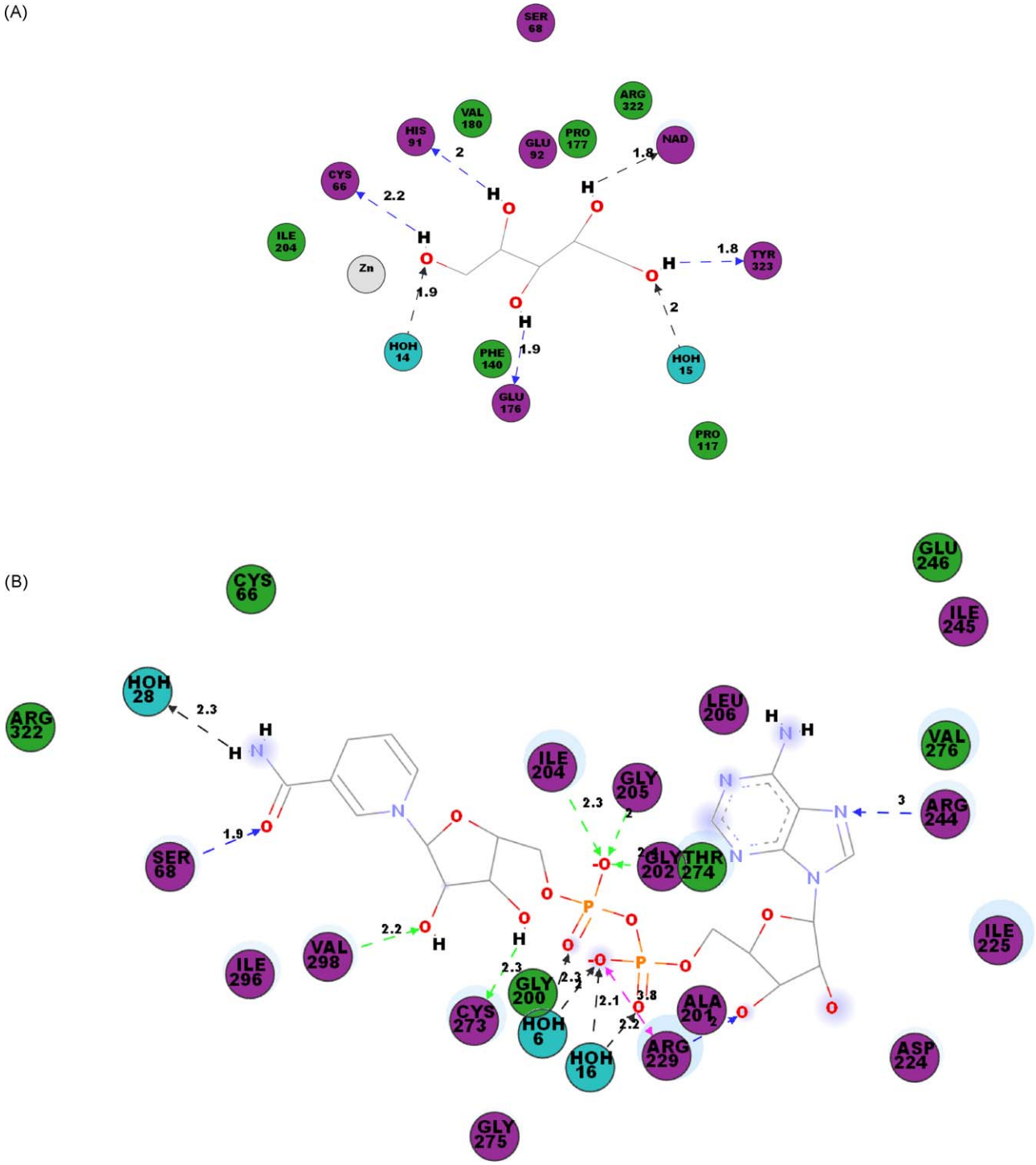

Fig. 4. 2D representation of the catalytic site and coenzyme binding domain of LAD1. (A) The binding mode of Zn^{2+} and the substrate in the catalytic site. (B) The interactions of LAD1 with NAD^+ in the coenzyme binding domain. The residues involved in various events are represented as following. Hydrogen bond, charge or polar interactions (magenta-colored circles), van der Waals (green circles), metal atoms (gray circles), water molecules (aquamarine circles), hydrogen-bond interactions with non-amino acid residues (black dashed line), charge interactions (pink dashed line), amino acid main chains (green dashed line), and amino acid side chains (blue dashed line). The distances shown are in Å.

3.8. Substrate binding

The molecular docking of the substrate L-arabinitol into the active site of the complex of LAD1, Zn^{2+} and NAD^+ revealed a possible interaction between LAD1 and L-arabinitol. Fig. 3A illustrates the residues present within 5 Å of L-arabinitol in the active site of the energy minimized LAD1 structure. The MD calculation revealed that all of the hydroxyl groups of the five-carbon sugar alcohol substrate were within the distance for hydrogen bonding. The C4 hydroxyl group of L-arabinitol interacted via hydrogen bonding (1.8 Å) with oxygen at C1 of the nicotinamide ring. The same OH group also formed an intramolecular H-bond (2 Å) with the C2 OH group of L-arabinitol. The C2 OH group was also involved in a H-bonding interaction with the catalytic residue His91 Nε (2 Å), and C1 OH group interacted with the sulfur group of Cys66 (2.2 Å) and a water (HOH14) molecule (1.9 Å). The C2 and C4 H-bonding network was the probable path for the hydride transfer that occurs in L-arabinitol oxidation. C3 and C5 coordinated with other catalytic residues, where C3 interacted with Glu176 OE1 (1.9 Å) and HOH14 (2 Å), while C5 interacted with Tyr323 (1.8 Å) and with a different water (HOH15) molecule (2 Å) (Fig. 3A). The 2D depictions of the interactions between these ligands, L-arabinitol (Fig. 4A) and NAD^+ (Fig. 4B) were generated. These depictions clearly enumerated the interactions, such as hydrogen bond or charge–charge interaction, between the surrounding residues and the ligands.

3.9. A possible mechanism of L-arabinitol oxidation

The analysis of the docked complex of LAD1 with NAD^+ and L-arabinitol allowed us to produce a model for the possible mechanism of substrate oxidation at a catalytic site. For most of the ADHs, the mechanism is ordered so that the coenzyme binds before the substrate [24]. For an alcohol substrate, the positive charge of NAD^+ contributed to the deprotonation of the alcohol proton and promoted binding to the active site Zn^{2+} ion. At the active site, the Zn^{2+} atom was tetra-coordinated by three protein side chains (Cys66, His92, Glu91) and a water (HOH14) molecule upon binding of the required cofactor NAD^+ and L-arabinitol. Both the C1 and C2 oxygen atoms of L-arabinitol bound to zinc, making the zinc pentavalent. The C3 and C5 carbon of L-arabinitol stacked in part against the nicotinamide ring which was consistent with the observed ordered mechanism. This study found that the C2 hydroxyl of L-arabinitol, which was oxidized by the enzyme to a ketose (L-xylulose), was hydrogen bonded with catalytic His91. The C2 carbon, which transferred its hydride to NAD^+ during the course of the reaction, was 3 Å from the nicotinamide C4, which was a suitable distance for the hydride transfer [25]. This investigation provided further insight into several aspects of the LAD1-catalyzed hydride transfer.

4. Conclusion

This is the first known report on the structural analysis of LAD1 based on the quaternary structure model of the L-arabinitol–LAD1 complex using MD simulations. The catalytic domain, coenzyme binding domain and the key residues involved in the catalytic event of LAD1 were determined. This study will hopefully facilitate a better understanding of the action mode of the ligand and guide further rational design studies. The interactions between the enzyme and the substrate proposed in this study are useful for understanding the potential mechanism of LAD1. Furthermore, as illustrated in this work, this approach will aid in the identification of the mutation sites that influence the enzyme activity. Predictions arising from these findings will stimulate further biochemical investigation and guide the design of enzymes to improve the utilization of sugar alcohols for the production valuable rare sugars.

Acknowledgements

This research was supported by a grant from the Korea Research Foundation (331-2007-1-D00144). This work was also supported by the 21C Frontier Microbial Genomics and Applications Center Program, Ministry of Education, Science & Technology, Republic of Korea.

Appendix A. Supplementary data

Supplementary data associated with this article can be found, in the online version, at doi:10.1016/j.jmgm.2010.01.004.

References

[1] M. Pail, T. Peterbauer, B. Seiboth, C. Hametner, I. Druzhinina, C.P. Kubicek, The metabolic role and evolution of L-arabinitol 4-dehydrogenase of *Hypocrea jecorina*, Eur. J. Biochem. 271 (2004) 1864–1872.
[2] P. Richard, J. Londesborough, M. Putkonen, N. Kalkkinen, M. Penttila, Cloning and expression of a fungal L-arabinitol 4-dehydrogenase gene, J. Biol. Chem. 276 (2001) 40631–40637.
[3] R. Sullivan, H. Zhao, Cloning, characterization, and mutational analysis of a highly active and stable L-arabinitol 4-dehydrogenase from *Neurospora crassa*, Appl. Microbiol. Biotechnol. 77 (2007) 845–852.
[4] T.A. Pauly, J.L. Ekstrom, D.A. Beebe, B. Chrunyk, D. Cunningham, M. Griffor, A. Kamath, S.E. Lee, R. Madura, D. McGuire, T. Subashi, D. Wasilko, P. Watts, B.L. Mylari, P.J. Oates, P.D. Adams, V.L. Rath, X-ray crystallographic and kinetic studies of human sorbitol dehydrogenase, Structure 11 (2003) 1071–1085.
[5] S. Kabsch, Dictionary of protein secondary structure: pattern recognition of hydrogen-bonded and geometrical features, Biopolymers 22 (1983) 2577–2637.
[6] A. Sali, L. Potterton, F. Yuan, H. van Vlijmen, M. Karplus, Evaluation of comparative protein modeling by MODELLER, Proteins 23 (1995) 318–326.
[7] G. Wu, D.H. Robertson, C.L. Brooks III, M. Vieth, Detailed analysis of grid-based molecular docking: A case study of CDOCKER-A CHARMm-based MD docking algorithm, J. Comput. Chem. 24 (2003) 1549–1562.
[8] R.E.B. Bernard, R. Brooks, Barry D. Olafson, David J. States, S. Swaminathan, Martin Karplus, CHARMM: a program for macromolecular energy, minimization, and dynamics calculations, J. Comput. Chem. 4 (1983) 187–217.
[9] M. Taufer, M. Crowley, D. Price, A.A. Chien, C.L. Brooks Iii, Study of a highly accurate and fast protein–ligand docking based on molecular dynamics, in: Parallel and Distributed Processing Symposium, 2004. Proceedings. 18th International, 2004, p. 188.
[10] M.G. Rossmann, D. Moras, K.W. Olsen, Chemical and biological evolution of nucleotide-binding protein, Nature 250 (1974) 194–199.
[11] A.M. Lesk, NAD-binding domains of dehydrogenases, Curr. Opin. Struct. Biol. 5 (1995) 775–783.
[12] S. Magesh, T. Suzuki, T. Miyagi, H. Ishida, M. Kiso, Homology modeling of human sialidase enzymes NEU1, NEU3 and NEU4 based on the crystal structure of NEU2: hints for the design of selective NEU3 inhibitors, J. Mol. Graph. Model. 25 (2006) 196–207.
[13] R.A. Laskowski, M.W. MacArthur, D.S. Moss, J.M. Thornton, PROCHECK: a program to check the stereochemical quality of protein structures, J. Appl. Crystallogr. 26 (1993) 283–291.
[14] R. Dai, M.R. Pincus, F.K. Friedman, Molecular modeling of cytochrome P450 2B1: mode of membrane insertion and substrate specificity, J. Protein Chem. 17 (1998) 121–129.
[15] R. Sanchez, A. Sali, Advances in comparative protein-structure modelling, Curr. Opin. Struct. Biol. 7 (1997) 206–214.
[16] B.L. Sibanda, T.L. Blundell, J.M. Thornton, Conformation of beta-hairpins in protein structures. A systematic classification with applications to modelling by homology, electron density fitting and protein engineering, J. Mol. Biol. 206 (1989) 759–777.
[17] J.F. Wang, D.Q. Wei, Y. Lin, Y.H. Wang, H.L. Du, Y.X. Li, K.C. Chou, Insights from modeling the 3D structure of NAD(P)H-dependent D-xylose reductase of Pichia stipitis and its binding interactions with NAD and NADP, Biochem. Biophys. Res. Commun. 359 (2007) 323–329.
[18] B.L. Vallee, F.L. Hoch, Zinc in horse liver alcohol dehydrogenase, J. Biol. Chem. 225 (1957) 185–195.
[19] D.S. Auld, T. Bergman, Medium- and short-chain dehydrogenase/reductase gene and protein families: The role of zinc for alcohol dehydrogenase structure and function, Cell. Mol. Life Sci. 65 (2008) 3961–3970.
[20] M.J. Banfield, M.E. Salvucci, E.N. Baker, C.A. Smith, Crystal structure of the NADP(H)-dependent ketose reductase from Bemisia argentifolii at 2.3 A resolution, J. Mol. Biol. 306 (2001) 239–250.
[21] U. Ryde, On the role of Glu-68 in alcohol dehydrogenase, Protein Sci. 4 (1995) 1124–1132.

[22] P.J. Baker, K.L. Britton, D.W. Rice, A. Rob, T.J. Stillman, Structural consequences of sequence patterns in the fingerprint region of the nucleotide binding fold. Implications for nucleotide specificity, J. Mol. Biol. 228 (1992) 662–671.
[23] C.A. Bottoms, P.E. Smith, J.J. Tanner, A structurally conserved water molecule in Rossmann dinucleotide-binding domains, Protein Sci. 11 (2002) 2125–2137.
[24] H. Theorell, Function and structure of liver alcohol dehydrogenase, Harvey Lect. 61 (1967) 17–41.
[25] H. Eklund, S. Ramaswamy, Medium- and short-chain dehydrogenase/reductase gene and protein families: Three-dimensional structures of MDR alcohol dehydrogenases, Cell. Mol. Life Sci. 65 (2008) 3907–3917.